3D Semi-Landmark based Statistical Face Reconstruction

Maxime Berar, Michel Desvignes, Gérard Bailly, Yohan Payan

3D Semi Landmarks-Based Statistical Face Reconstruction

Maxime Berar[1], Michel Desvignes[1], Gérard Bailly[2] and Yohan Payan[3]

[1] Laboratoire des Images et des Signaux, Saint Martin d'Hères, France
[2] Institut de la Communication Parlée, Grenoble, France
[3] Laboratoire TIMC/IMAG, Faculté de Médecine, La Tronche France

The aim of craniofacial reconstruction is to estimate the shape of a face from the shape of the skull. Few works in machine assisted facial reconstruction have been conducted so far, probably due to technical (poor machine performance and data availability) and theoretical (complexity) reasons. Therefore, the main works in the literature consist in manual reconstructions. In this paper, an original approach is first proposed to build a 3D statistical model of the skull/face set from 3D CT scans. Then, a reconstruction method is introduced in order to estimate, from this statistical model, the 3D facial shape of one subject from known skull data.

Keywords: facial reconstruction, statistical model, elastic registration, missing data reconstruction

1. Introduction

Craniofacial reconstruction is usually considered when confronted with an unrecognizable corpse and when no other identification evidence is available. In such cases, the skeletal remains are the only available information for creating a picture of that person. The aim of craniofacial reconstruction is then to produce a likeness of the face using the skeletalized remains. This reconstruction may hopefully provide a route to a positive identification.

Several 3D manual methods for facial reconstruction have been developed up to now and are currently used in practice. They consist of modeling a face on the remaining skull by use of clay and plasticine. However, manual reconstruction methods have several fundamental shortcomings, such as being highly subjective, time-consuming and requiring artistic talent. Computer-based methods have been developed to try to complement or even provide an answer to these shortcomings.

Some current machine aided techniques fit a template skin surface to a set of interactively placed virtual dowels on a 3D digitized model of the remaining skull [1] – [5]. Other works propose to deform a reference skull in order to match the remaining skull, thanks to crest lines (lines of maximal local curvature) [6], control data sets [7] or feature points [8]. Then they apply an extrapolation of the calculated skull deformation to the template skin surface associated to the reference skull. For both techniques, the template skin or reference skull can either be a generic surface or a specific best look-alike according to the skull. However, the facial reconstruction is biased by the choice of the reference skull and the template skin. Recent works using multiple reference skulls [9], or a combined statistical deformable model of facial surfaces and tissue thickness [10] both addressed the facial reconstruction problem and discussed these biases.

Several works have addressed the problem of construction of statistical models. Input data are first registrated in a common reference system by minimization of a cost function. Then, the model, often based on PCA, is computed. The cost function can be modeled on voxel intensities, [11], voxel labels [12], manual landmarks [13], features [14], or nearest points [15] in 2D images or 3D density maps. In craniofacial reconstruction, two objects, the skull and the skin, have to be registrated. It is of utmost importance that the registration method does not modify the relationship between these objects. Most methods based on voxel intensities use an implicit model of elastic deformation in the cost function, which can biais the relationship between skin and skull objects in the registrated image. Other methods often use meshes to represent surfaces in 3D. The meshes must have the same connectivity (same number of vertices and same relationships among them) to build a statistical model. This is achieved by a parameterization of the object [16], by an optimization of the resulting statistical model [17], or by constructing template references [18]. In [12], the authors decimate the meshes to reduce the influence of noise and the processing time. Our model is closely related to these last methods [17, 18] and also follows tracks from [20] where the model is built from labeled images.

In this paper, a method to build a joint statistical 3D model of the skull and face is presented. This model is then used to reconstruct a face from available skull data. The idea is similar to [6-8] but uses a statistical shape model of both the skull and the face for the reconstruction task, instead of a sole extrapolation of the deformation field. A 3D-to-3D matching procedure propagates pseudo-landmarks from reference surfaces to the various surfaces of the skull and face of our database. Therefore, when applied to several individuals, a statistical model of the cross-variability of the skull and the face is built. The reconstruction of the face is then solved using the direct statistical relationship between skin and skull surface shapes given by the model. Face reconstruction can therefore be seen as a missing data problem.

This paper is organized as follows. Section 2 describes the elaboration of the normalized skull and face geometries obtained by a 3D-to-3D matching procedure. Section 3 presents the statistical model built upon the normalized faces and skulls. Finally, section 4 introduces the facial reconstruction method and presents results. Some open research lines for further improvements are also presented.

2. Skull and Face Database

2.1. Method

An entry (i.e. a sample) in our database consists of a skull surface coupled with a skin surface. For facial reconstruction, only the skull surface is known. These surfaces are represented by 3D meshes (vertices and triangles). In order to construct the statistical model, each skull or skin shape must share the same mesh connectivity. This particular connectivity arises from a subject-shared reference mesh (also denoted as generic mesh in the following). For each individual in our database, original meshes are reconstructed from CT data of the subject (Figure 1). Each of these subject meshes has its own connectivity. The main problem is then to establish correspondences between the different meshes of the training set, so as to match the anatomically equivalent features. Each of these subject meshes needs to be registrated in the subject-shared reference system. Like Fleute et al. [21] correspondence is established by elastic registration of template shapes (mandible, skull and face) with all the subject shapes (Figure 2). Joint propagation of mesh connectivity and geometry is performed from the generic mesh to match the subject shapes. The triangles for a region of the skull or the face are therefore supposed to be the same for all samples, while the variability of the position of the vertices will reflect the anatomical characteristics of each sample. These vertices can be considered as semi-landmarks (or pseudo-landmarks), i.e. points that do not have names but that match across all the samples of a data set under a reasonable model of deformation [22]. As each skull or skin shape (also denoted as subject-specific generic meshes) share the same mesh connectivity, a statistical model can be built (Figure 3).

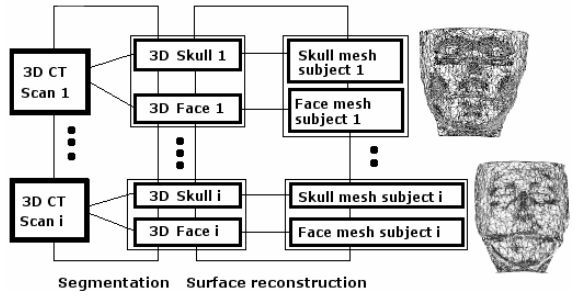

Figure 1. Generation of the subject meshes.

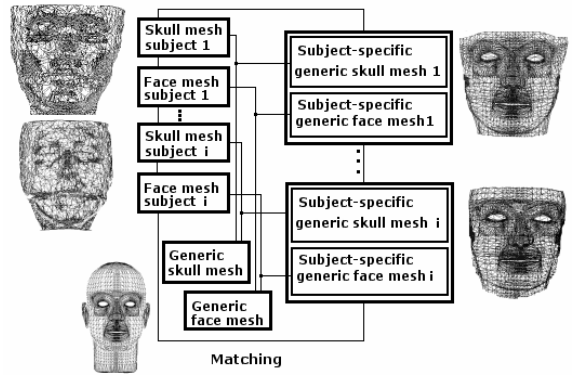

Figure 2. Generation of the subject-specific generic meshes.

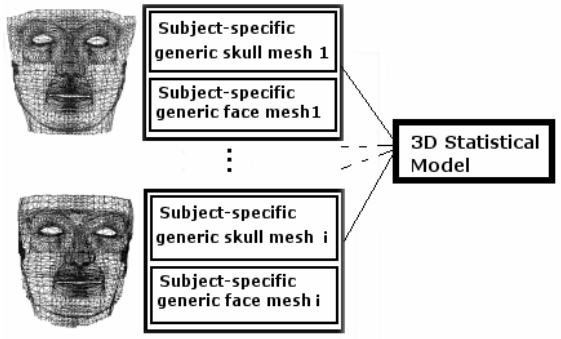

Figure 3. Building the statistical model from the subject-specific generic meshes.

Figure 4. (Top) 3D raw scan data (only axial slices were collected; midsagital and coronal have been reconstructed here by image processing), (Bottom) subject-specific mesh reconstructed using the marching cube algorithm [23]

2.2. Generation of Subject Meshes

Axial CT slices (see Figure 4) were collected for the partial skulls and faces of 15 subjects (helical scan with a 1-mm pitch and slices reconstructed every 0.31 mm or 0.48 mm). Since these data were collected during regular medical exams, excitation of the brain volume was avoided if not necessary. So nearly all the skull are partially scanned, and only two complete skull and face volume data were available. Bones and skin image volumes are first separated using intensity thresholding and morphological operators. Face volumes are then filled up, with metal artefacts if any being manually removed. The mandible and the skull have to be separated during the segmentation process because the subjects have different mandible apertures. Skull and mandible are semi-manually separated using seed-growing regions. At the end of the segmentation process, three binary volumes are obtained. The subject meshes are reconstructed for each volume (face, skull, mandible) using a standard Marching Cube algorithm [23] and a smooth decimation algorithm is applied to the resulting meshes [24]. Each subject shapes are now described with a different connectivity. Moreover, undesired holes (such as the orbita wall, foramina, etc.) are still present in the subject meshes.

2.3. Subject-specific generic meshes generation

Subject-specific generic (SSG) meshes are obtained by matching the subject meshes with generic meshes. Generic meshes (see Figure 5) have been taken from the Visible Woman Project [25] (skull, 3473 verts, and mandible, 1100 verts) and from [26] (face, 5828 verts). These meshes have been semi-manually obtained by their respective authors. The vertices of these meshes are located on crest lines and in [26] they are regularly distributed following facial animation needs. Moreover each of these generic meshes has no undesired holes.

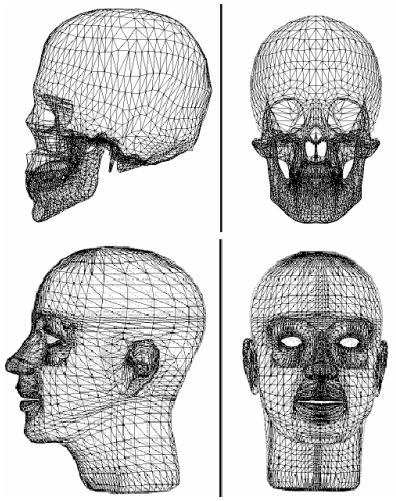

Figure 5. Skull mesh from [25] (Top) and face mesh from [26] used as generic meshes (Bottom)

The matching procedure we use is the same as described in [27]: the elastic registration of the generic meshes to the subject meshes uses the matching algorithm proposed by Lavallée et al. [28] with a minimisation of the distances between the two shapes. It basically consists of the deformation of the initial 3D space by several trilinear transformations. These transformations are applied to all vertices of elementary cubes of the generic mesh towards the subject mesh. The problem of matching symmetry [12] is encountered, due to the vertices density dissimilarity between the subject and generic meshes. Indeed, the number of vertices is 30 to 70 times larger in the subject meshes than in the subject-specific meshes. Therefore, a symmetrized minimization function is used [29].

The distance computed for the quantitative analysis of the SSG and subject meshes is a point-to-surface distance from the subject-specific generic meshes to the subject meshes.

Maximal matching errors between the SSG mandible meshes and the subject mandible meshes are located on the teeth and on the coronoid process. The mean distance can be considered as the registration noise, partly due to the density dissimilarity (see Table 1.). Teeth will not be part of our model, due to the frequent metal artefacts in CT scans.

Subject skull meshes are registered on the corresponding parts of the generic skull mesh, as most of the skulls were partially scanned. The maximal matching errors in the resulting SSG skull meshes are located in the spikes beneath the skull, where the individual variability and the surface noise are large due to segmentation errors. Only the minimum common

subset of shapes will be used to build the statistical model (Figure 6).

Finally, SSG face meshes are obtained using the same procedure. In this case, the maximal matching errors between SSG and subject meshes are located around the eyes, that are part of the original data, but not part of the generic mesh (see Figure 7 for a distance map between a SSG mesh and a subject mesh).). Again, only the minimum common subset of shapes will be used to build the statistical model. Figure 8 shows the 15 normalized shapes of the common subset of the face database.

Table 1. Distance between the subject (subject CT data reconstructed through Marching Cube) and the subject-specific generic meshes.

Distances (mm)	mean	Max
Mandible	2	8
Skull	4	36
Face	1	5

The 15 subjects are now registrated in a common shape space. These subset meshes have 3780 face vertices and 2900 skull vertices.

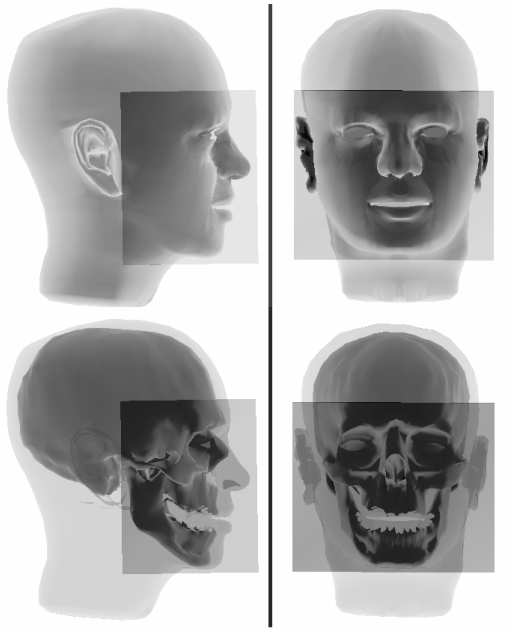

Figure 6. Minimum common subset of shapes used to build the statistical shape model.

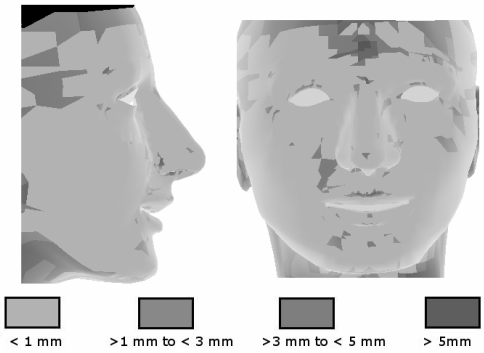

Figure 7. Distance map of a SSG face mesh to a subject mesh.

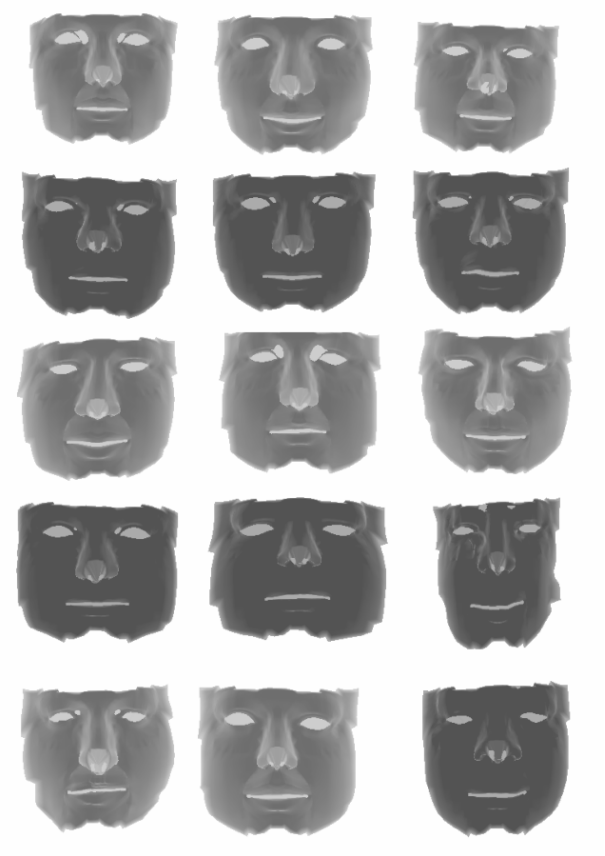

Figure 8. The 15 face subsets forming the database

//// a refaire avec les modèles plus complets (nez/cou)

3. Statistical Modelling

3.1. Building the statistical model

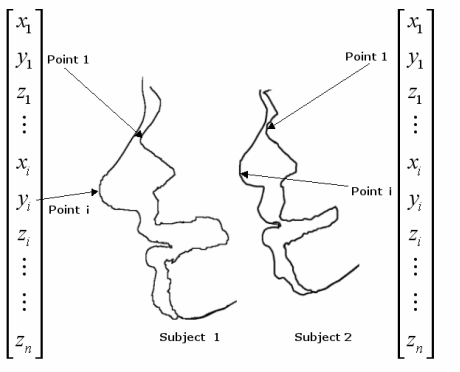

Figure 9. Each vertex of the subject-specific generic meshes is considered as being at the same location reflecting thus the inter-individual variations of shape.

Each vertex of the SSG mesh is supposed to be a semi-landmark of the 3D surfaces – see Figure 9 – reflecting thus the inter-individual variations of shape. The statistical model is based on this assumption and is computed on the minimum common subset of the original data. The 15 matched skulls and faces are first fitted on the mean configuration of the skull using Procrustes normalization [30]. Seven degrees of freedom due to initial location and scale are retrieved by this fit (three due to translation along the axes, three due to rotations, one for scale adjustment). As the fitting is based on mean skull configuration, the relationships between each face and skull are conserved. A statistical model of the subset of skulls and faces is then built using Principal Component Analysis (PCA). The result of the PCA is a geometrically averaged skull and face template, which is computed together with a correlation-ranked set of modes of principal variations based on inter-subjects variations.

Let $\{T_i; i = 1 \cdots l\}$ denote l shapes (l=15). Each shape $T_i = (x_{i1}, y_{i1}, z_{i1}, ..., y_{in+m}, z_{in+m}) \in R^{3(n+m)}$ consists of the 6680 vertices (n=2900 skull verts., m=3780 face verts.) of the subset of meshes. Using PCA, we can write :

$$T = \tilde{T} + \Phi b \qquad (1)$$

where $\tilde{T}$ is the average shape vector, Φ is a matrix whose columns are the eigenvectors of the covariance matrix S of the centered data and b is the shape parameter vector of the model. If Φ contains the $t < \min\{l, 3(m+n)\}$ eigenvectors corresponding to the largest nonzero eigenvalues of S, we can approximate any shape of the training set using (1), where $\Phi = (\phi_1 | ... | \phi_t)$ and b is a t-dimensional vector given by $b = \Phi^t (T_i - \overline{T})$. Any points of the training set can be represented or retrieved with the t values of the vector b by $T \approx \tilde{T} + \Phi b$.

By varying the parameters b, different instances of the skull and face can be generated. Assuming that the cloud of the meshes vertices follows a multidimensional Gaussian distribution and that shape parameters ly within the statistical boundaries of the model, the skulls and faces generated by varying the shape parameters are similar to those contained in the training set, resulting in new synthetic but plausible skulls and faces.

3.2. Results

In our case, with 15 subjects, a total of 13 variations modes can be computed, since a leave-one-out approach is used to test the generalization of the modeling procedure. Only the first eight modes of variations (see Table 2) are significant in terms of represented variance.

Table 2. Percentage of cumulative variance explained.

Mode number	1	2	3	4	5	6	7	8
Cumulative variance	36	51	64	73	79	84	88	91

The accuracy of this model is tested by reconstruction: for a given mesh, variation modes (b) are computed by minimization of the distance between the true real mesh (T) and the reconstructed mesh ($\tilde{T}+\Phi b$). The mean reconstruction errors (Figure 10) for the last three modes are below the millimeter for samples of the learning database. So the reconstruction is quite accurate with samples in the learning database. Reconstruction error for a test sample i.e. a sample which is not in the learning database, is around 3.85 mm for the skull and 3.25 mm for the face using the first four modes. The skull reconstruction is mostly determined by the first variation as the reconstruction error is then around 4.2 mm. These two results demonstrate that this method seems promising but that the number of samples in the learning database is too small.

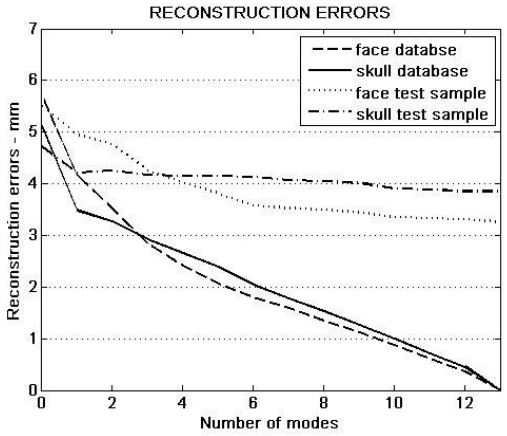

Figure 10. Mean reconstruction errors of the skull and face using an increasing number of modes

Except for the first variation mode, the principal variations of the shape explained by the model are a little more descriptive of the variation of the face shape than those of the skull shape. It can be linked to the greater number of vertices belonging to the face (3780) than to the skull (2900) (Table 3).

Table 3. Percentage of cumulative variance explained for each part of the model (face, skull) for the first 6 modes.

Mode number / Cumulative variance	1	2	3	4	5	6
face	36	50	64	75	82	86
skull	39	48	59	66	72	79

Figure 11 and 12 present the variations of the skull and face shapes according to the first modes for parameters varying between +3 and –3 times the standard deviation. The first parameter influences variations of the face and skull width, while the second parameter models the face and skull height. The third parameter acts upon the shape of the nose as well as the ratio between the upper and the lower parts of the face. Parameter four influences the shape of the nose and parameter five is linked to the shape of the jaw. The first five modes of variations represent 73 percents of the cumulative variance (Table 2). As the mandible position is different for each subject, each mode of variation models also the jaw aperture (Figure 12).

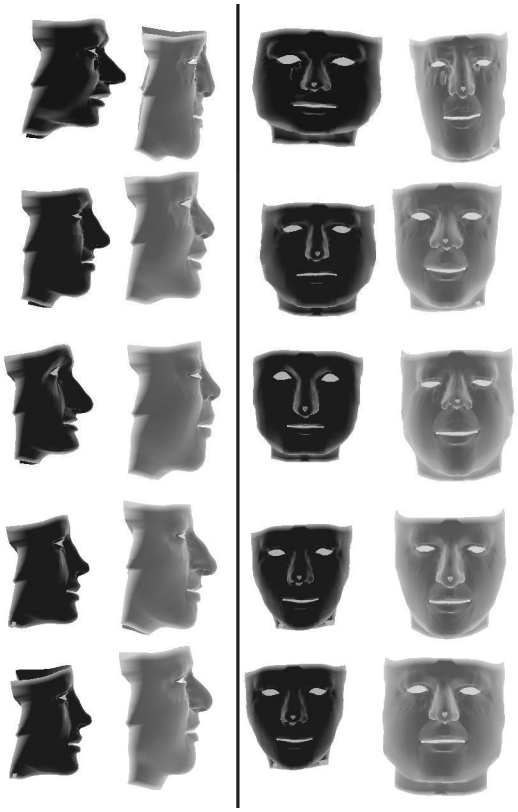

Figure 11. Variations of the face shape according to the first 5 modes for parameters varying between +3 and –3 times the standard deviation.

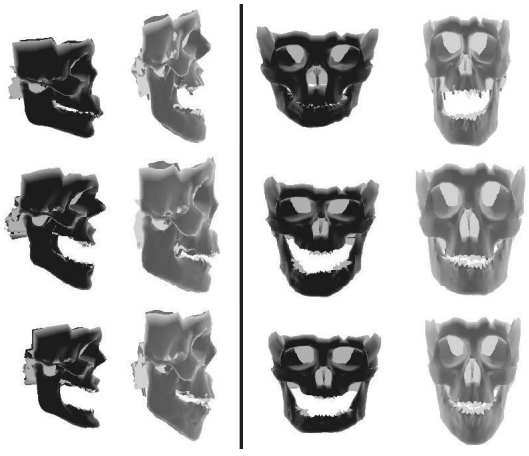

Figure 12. Variations of the skull shape according to the first 3 modes for parameters varying between +3 and –3 times the standard deviation.

4. Statistical Reconstruction

4.1. Missing Data Extension

The linear PCA model can be extended in an elegant way in order to take into account spatial relations between landmarks and to estimate an unknown part of a partially visible or occluded model [31].

$$\begin{bmatrix} C_1 \\ \vdots \\ C_n \\ X_1 \\ \vdots \\ X_m \end{bmatrix} = \begin{bmatrix} \overline{C}_1 \\ \vdots \\ \overline{C}_n \\ \overline{X}_1 \\ \vdots \\ \overline{X}_m \end{bmatrix} + \begin{bmatrix} \Phi_{1,1} & \cdots & \Phi_{1,n+m} \\ \vdots & \ddots & \vdots \\ \Phi_{n+m,1} & \cdots & \Phi_{n+m,n+m} \end{bmatrix} \begin{bmatrix} b_1 \\ \vdots \\ b_n \\ b_{n+1} \\ \vdots \\ b_t \end{bmatrix}$$

Under this hypothesis, if some points (says n points) are known, the remaining unknown points (says m points) are determined using PCA. The shape parameter vector b (of dimension $t = n+m$) will also be determined. Without any approximations, we can write the unknown vector $(b_1,\ldots,b_t,X_1,\ldots,X_m)$ in the following system:

$$\begin{bmatrix} C \\ 0 \end{bmatrix} = \begin{bmatrix} \Phi_C & 0 \\ \Phi_X & -Id \end{bmatrix} \begin{bmatrix} b \\ X \end{bmatrix} \quad or \;\; T = MZ$$

$$where\ \Phi_C = \begin{bmatrix} \Phi_{1,1} & \cdots & \Phi_{1,t} \\ \vdots & \ddots & \vdots \\ \Phi_{n,1} & \cdots & \Phi_{n,t} \end{bmatrix} \qquad (2)$$

$$and\ \Phi_X = \begin{bmatrix} \Phi_{n+1,1} & \cdots & \Phi_{n+1,t} \\ \vdots & \ddots & \vdots \\ \Phi_{n+m,1} & \cdots & \Phi_{n+m,t} \end{bmatrix}$$

This is a linear system with $n+m$ equations and $n+2m$ unknowns that can not be resolved. Since PCA can represent the dataset with $t < n+m$ values, if we suppose $t=n$, the system has a direct solution. Notice, that if we choose t<n, the system becomes overdetermined and a least square method can be used to resolve the system :

$$\min \left\| \begin{bmatrix} C \\ 0 \end{bmatrix} - \begin{bmatrix} \Phi_C & 0 \\ \Phi_X & -Id \end{bmatrix} \begin{bmatrix} b \\ X \end{bmatrix} \right\|^2$$

The cost function is :

$$J(b,X) = \begin{bmatrix} C - \Phi_C * b & -X + \Phi_X * b \end{bmatrix} \begin{bmatrix} C - \Phi_C * b \\ -X + \Phi_X * b \end{bmatrix}$$

In matricial form, J can be rewriten as :

$$\begin{aligned} J(Z) = J(b,X) = \left\| T - M * Z \right\|^2 = \\ \left(T'T - T'MZ - Z'M'Y + Z'M'MZ \right) = \\ \left(T'T - 2T'MZ + Z'M'MZ \right) \end{aligned} \qquad (3)$$

As the matrix $[\Phi_C\ \Phi_X]'$ is an orthonormal basis, $M'M$ takes the following form and the cost function becomes:

$$M'M = \begin{bmatrix} \Phi_C' & \Phi_X' \\ 0 & -Id \end{bmatrix} \begin{bmatrix} \Phi_C & 0 \\ \Phi_X & -Id \end{bmatrix} = \begin{bmatrix} Id & -\Phi_X' \\ -\Phi_X & Id \end{bmatrix} \qquad (4)$$

$$J(b,X) = C'C - 2b'\Phi_C'C + X'X - 2b'\Phi_X'X + b'b$$

The derivatives with respect to X and b are null :

$$\frac{\partial J(b,X)}{\partial b} = -2\Phi_C'C + 2b - 2\Phi_X'X = 0 \qquad (5)$$

$$b = \Phi_C'C + \Phi_X'X$$

$$\frac{\partial J(b,X)}{\partial X} = -2\Phi_X b + 2X = 0 \qquad (6)$$

$$X = \Phi_X b$$

Reporting (6) in (5), the solution is :

$$\begin{aligned} b &= \left(Id - \Phi_X'\Phi_X \right)^{-1} \Phi_C'C \\ X &= \Phi_X \left(Id - \Phi_X'\Phi_X \right)^{-1} \Phi_C'C \end{aligned} \qquad (7)$$

Note that (Id-Φ_X'Φ_X) is always invertible, since it is a symmetric positive defined matrix.

In this framework, a linear approximation of spatial relations between known and unknown points is explicitly determined from the eigenvectors of the covariance matrix. The determination of the unknown points is in fact the determination of the shape parameters given the known points (6). The determination of the shape parameters can be linked to the influence of each part on each shape parameter, described by Φ_C and Φ_X. As Φ_C and Φ_X depend only of the training set, new models must be build to act upon Φ_C and Φ_X . One way is to build a new model with a larger (or smaller) training set. One other way is to change the ratio between each part.

4.2. Results : Synthetic Data

A synthetic skull and face database is first built using one of the original individuals and a set of elastic transformations defined as an octree. Random transformations of the cube enclosing the two meshes were provided, thus transforming the two meshes. Five parameters are used to deform the meshes: three scaling parameters, and variations of the center of the X face and of the central axis of the cube (Z direction). Of

course, these variations do not simulate the reality of the skulls and faces variability. However, it is a way to artificially verify the missing data formulation and the semi-landmark hypothesis.

Using the extension of the linear PCA defined above, the face of a synthetic subject can be reconstructed from his skull and from the statistical model built using synthetic data. The known part (Ci) contains the skull vertices while the unknown part (Xi) contains the face vertices.

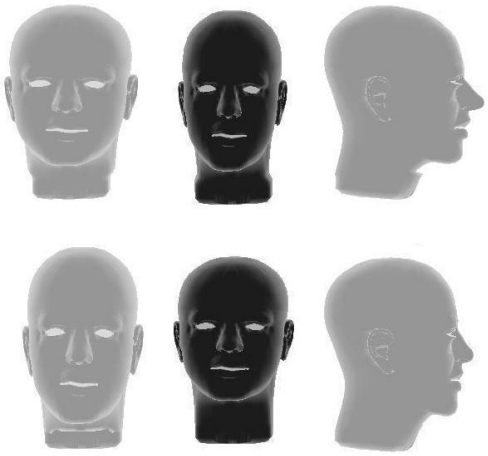

Figure 13.Examples of synthesis meshes.

A set of one hundred meshes is generated using these random transformations (see Figure 13 for examples of generated faces). To further increase the variability on the face, a Gaussian noise is added to each point. The level of this noise (2 mm) is chosen so that we still remain in the semi-landmark paradigm. Indeed, a large level of noise could change the relative positions of the vertexes of the mesh, thus making the concept of semi-landmark not valid anymore.

Figure 14 and 15 plot the reconstruction results.. Test samples are reconstructed with a mean accuracy of 1 mm. The missing data error is in the same range. It is important to note that the missing data error converges to the reconstruction error for the known part of the test sample (the skull) as well as for the unknown part (the face. If the subject-specific meshes are used as test samples on the synthesis database, bad reconstructions are obtained for each individual as the variations of the shapes used are too simple

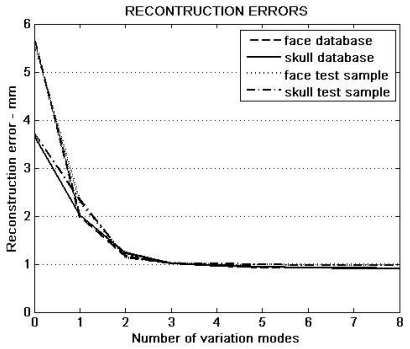

Figure 14. Mean reconstruction errors of the skull and face using an increasing number of mode for the synthetic database model.

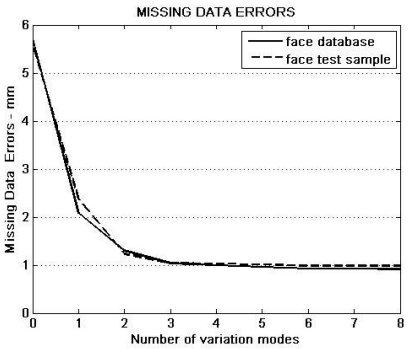

Figure 15. Mean Facial Reconstruction errors using an increasing number of modes for the synthetic database model.

4.3. Statistical Facial Reconstruction

The face of a subject can be reconstructed from his skull and from the statistical model defined previously (in 3.2), using the missing data extension of the model. The known part (Ci) contains the skull vertices while the unknown part (Xi) contains the face vertices.

Again, a leave-one-out approach is used to test the accuracy of the facial reconstruction. The learning database is composed of all subjects minus one, which is the test sample. Every subject becomes the test sample in turn. Figure 16 gives the mean reconstruction error of the test sample. It also gives the reconstruction error for the samples of the learning database.

In all cases, the global reconstruction is correct. The face and skull are reconstructed with an accuracy of 0.5 mm for the samples in the learning database. Test face sample is reconstructed with a mean accuracy of 6 mm. Clearly, these results show that the method is promising but suffers from the size of the learning database. The first parameter offers a better approximation of the reconstructed face with a mean reconstruction error of 5.2 mm. As the skull provides essentially the first mode of variation (see figure 10) and the other modes are

mostly related to variations of the face for our test sample, only the performance for the first parameter should be considered. For each additional variation mode, the prediction should not be considered as it infers variations of the face from variations not taken into account for the skull, the values of the variations modes being not accurate. As these parameters do not correspond to variation modes with null eigenvalues, a large error in their prediction results in a large error in reconstruction.

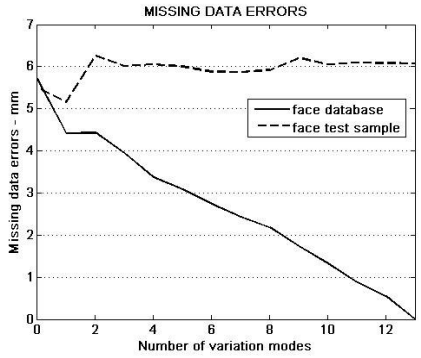

Figure 16. Mean Facial Reconstruction errors using an increasing number of modes.

The repartition of the missing data errors on the face is shown figure 17. Large errors are located on the cheeks, on the neck and on the sides of the nose. It is important to note that the cheeks are not attached to the skull and that the database provides different mandible positions. So, it is very difficult to predict correctly the position of the vertexes of the cheeks. Moreover, the density of vertexes for the cheeks region is quite low, which authorizes a possible sliding of those points on the skin surface. The neck is unconnected to the skull, so large errors are inescapable. Finally it is known that the prediction of the shape of the nose from the shape of the skull is very difficult [32, 33]. The links between the two organs are complex. These errors located on the sides of the nose are probably due to this lack of regularity. The good reconstruction of the tip of the nose can be conversely associated to the template used during the creation of the database.

When using a smaller bounding box that excludes the tip of the nose and the neck, we gain half a millimeter in the accuracy of the prediction (to 4.6 mm). The maximal error is reduced to 3 mm as seen in figure 18.

Two limitations of the current database are its small size, the non homogeneity of the face mesh (the regions of the nose and the lips are much more dense than the rest of the mesh) and the coarseness of the skull mesh. The following section presents a way of compensating for these limitations. Using a decimated mesh of the face (with a more homogenous distribution of the vertices), we indirectly give more weight to the skull vertices in the statistical model. The skull is then more accurately parameterised by the model and errors on the estimation of the skull shape interfere less on the prediction of the face.

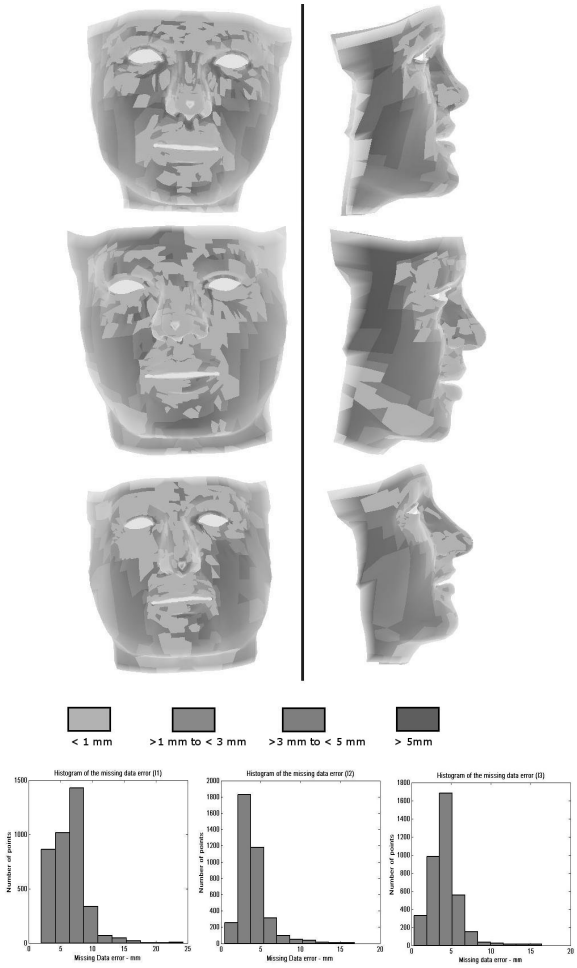

Figure 17 : Distance maps and histograms of the facial reconstruction error for 3 reconstructed faces.

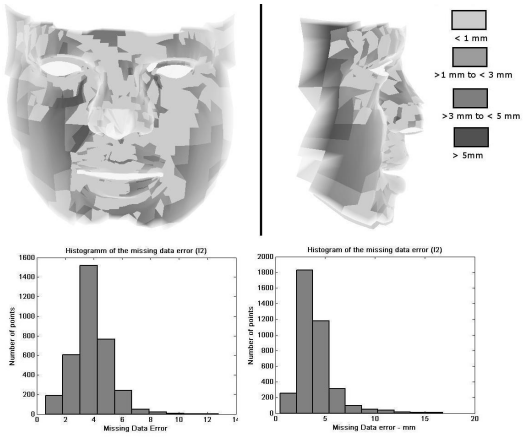

Figure 18. Distance maps and histograms of the facial reconstruction error for a reconstructed face using the enclosed model (no neck or tip of the nose) (left) and the original model (right).

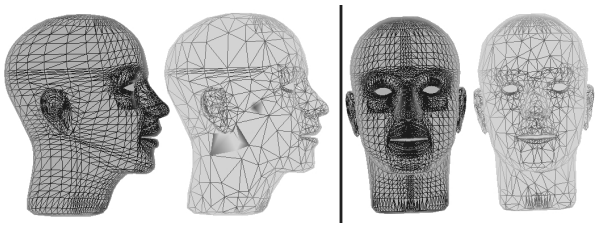

Figure 19. Original and decimated face meshes.

4.4. Decimated Facial Reconstruction

A decimated face mesh (929 vertices) is extracted from the original mesh (3780 vertices). As the decimated mesh is a subpart of the original mesh, every entry of the database can be expressed with only the vertices belonging to the decimated mesh. Each vertex of the decimated mesh represents a larger area of the face. The skull vertices now represents 75% of the vertices of the model. They have now more influence on the eignevectors emerging from statistical modelling.

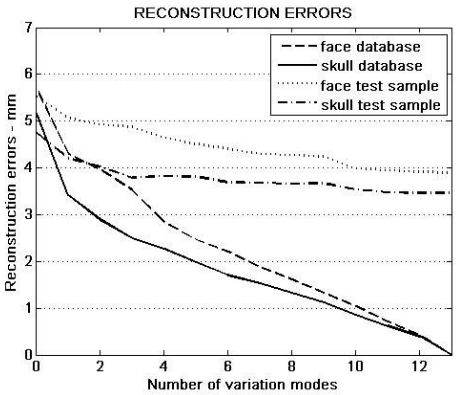

Figure 20. Mean reconstruction errors of the skull and face using an increasing number of mode for the decimated model.

The accuracy of this decimated model is first tested by global reconstruction. The mean reconstruction errors (figure 20) for the last three modes are below the millimeter for samples of the learning database as with the original mesh. The reconstruction is quite accurate with sample in the learning database. Reconstruction error for a test sample is around 3.6 mm for the last four modes. These results are similar to those of the non-decimated mesh. The reconstruction of the skull test sampled is now determined essentially by the first three modes of variations: the cumulative explained variance is now more descriptive of the skull shape variations than the face shape variations (Table 4).

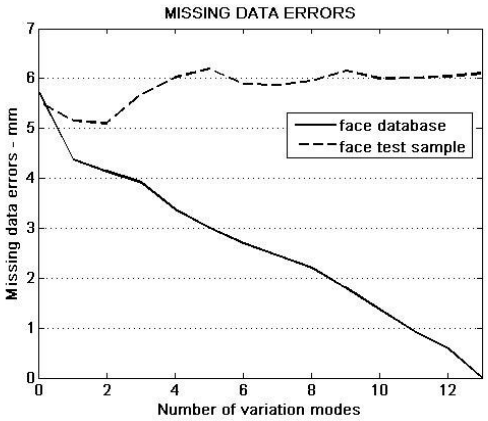

Figure 21. Mean Facial Reconstruction errors using an increasing number of modes for the decimated model

Table 4. Percentage of cumulative variance explained for each part of the model (face, skull) for the first 6 parameters.

Mode number / Cumulative variance	1	2	3	4	5	6
Face + skull	38	55	65	72	78	83
face	31	40	50	63	71	76
skull	41	59	68	72	78	83

Here again, the reconstruction of the face using the missing data extension of the PCA is promising (figure 21). The face is reconstructed with an accuracy of 0.6 mm for the samples in the learning database. Test samples are reconstructed with a mean accuracy of 6.0 mm. As with the original model, the first variation mode offers a better approximation of the reconstructed face with an error of 5.1 mm. But now the second parameter also gives an adequate information for the prediction of the face. The distribution on the face of the facial reconstruction error is similar to the original model (see figure 22).

In conclusion, the "decimated" model gives similar results to the "global" model (the gain is 0.1 mm for the facial reconstruction with 2 valid modes). However these results show that the more accurately the skull will be parameterised by the model (i.e. the greater the number of valid variation parameters), the more accurately the face will be predicted, as the error on these parameters determining the skull will not interfere on the prediction of the face.

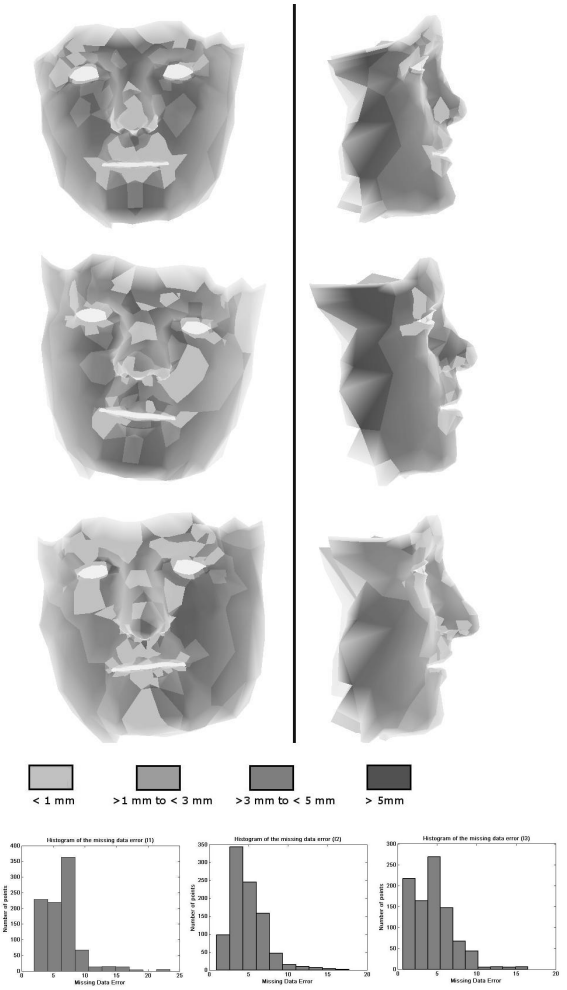

Figure 22. **Distance maps and histograms of the facial reconstruction error for 3 reconstructed decimated faces.**

5. Conclusion

In this paper, a face and skull statistical model is proposed for 3D machine-aided facial reconstruction. To build this statistical model, a 3D-to-3D matching procedure delivers subject-specific meshes of the skull and face with the same number of vertices. A shared normalized space for the faces and skulls is therefore built. The direct statistical relationships between the face and the skull included in the statistical model are used to reconstruct the missing data of the face when the skull is the only available information. For this, a missing data extension of the Principal Component Analysis is used.

Results are visually correct and mean measured errors show that the method is promising as it will be probably more efficient for larger learning database. One way of increasing the efficiency of the model is presented. It consists in decimating the face mesh in order to adjust its density to the skull mesh density, thus giving a higher weight to the known part of the problem, i.e. skull data. The corresponding results are similar to the ones provided by the original model (at least in term of facial reconstruction), but a slightly more efficient modeling of the skull was observed.

We will test this statistical approach using data acquired with a more adequate experimental protocol and using data from subjects with varied age and sex. The approach presented here may be extended towards relevant covariation between shape and appearance as well as between shape and range of motion. Aestehetic and rehabilitation surgery may thus also benefit from such anatomy-aware and subject-informed statistical models.

Acknowledgment

CT scans data have been collected for several subjects thanks to the maxillofacial department of Toulouse Hospital, with a grant from the BQR/INPG “Vésale”. We acknowledge Praxim-Medivision SA for the use of the initial 3D-to-3D matching software.

References

[1] P. Vanezis, Application of 3-D computer graphics for facial reconstruction and comparison with sculpting techniques.” Forensic Science International, 42 (1989), pp. 69-84.

[2] P. Vanezis, M. Vanezis, G. McCombe, T. Niblet, Facial reconstruction using 3-D computer graphics. Forensic Science International, 108 (2000), pp. 81-95.

[3] R. Evenhouse, M. Rasmussen, L. Sadler, Computer-aided Forensic facial reconstruction. Journal of BioCommunication, 19.2 (1992), pp. 22-28.

[4] A.W. Shahrom, P. Vanezis, R.C. Chapman, A. Gonzales, C. Blenkinsop, M.L. Rossi, Techniques in facial identification : computer-aided facial reconstruction using laser scanner and video superimposition. International Journal of Legal Medicine, 108 (1996), pp. 194-200.

[5] A. J. Tyrell, M.P. Evison, A.T. Chamberlain, M.A. Green, Forensic three-dimensional facial reconstruction : historical review and contemporary developments. Journal of Forensic Science 1997; vol. 42(4): pp. 653-661.

[6] G. Quatrehomme et al, A fully three-dimensional method for facial reconstruction based on deformable models. Journal of Forensic Science, 42.4 (1997), pp. 649-652.

[7] L.A. Nelson, S.D. Michael, The application of volume deformation to three dimensional facial reconstruction : a comparison with previous techniques. Forensic Science International, 94 (1998), pp. 167-181.

[8] M.W. Jones, Facial reconstruction using volumetric data. Proceedings of the 6th International Vision Modeling and Visualisation Conference, (2001), pp. 21-23, Stuttgart, Germany.

[9] D. Vandermeulen, P. Claes, P. Suetens, S. De Greef, G. Willems, Volumetric deformable face models for cranio-facial reconstruction. Proceedings of the 4th international symposium on image and signal processing and analysis - ISPA, (2005), pp. 353-358, Zagreb, Croatia

[10] P. Claes, D. Vandermeulen, S. De Greef, G. Willems, P. Suetens, Statistically deformable face models for cranio-facial reconstruction. Proceedings of the 4th international symposium on image and signal processing and analysis - ISPA, (2005), pp. 347-352, Zagreb, Croatia.

[11] R. P. Woods, S. T. Grafton, , C. J., Holmes, S. R. Cherry and J. C. Mazziotta, Automated image registration: I. General methods and intrasubject, intramodality validation. Journal of Computer Assisted Tomography, 22 (1998), pp :141-154.

[12] A. D. Brett and C. J. Taylor, A method of automated landmark generation for automated 3D PDM construction. Image and Vision Computing, 18.9 (2000), pp 739-748.

[13] Bookstein, F. L. 1991. Morphometric tools for landmark data. Cambridge Press. 435 pp.

[14] G. Subsol

[15]V. Blanz, A. Mehl, T. Vetter, H.-P. Seidel, A Statistical Method for Robust 3D Surface Reconstruction from Sparse Data. 3DPVT, (2004), pp 293-300.

[16] C. Brechbühler, G. Gerig, O. Kübler, Parameterization of Closed Surfaces for 3-D Shape Description. CVGIP: Image Understanding, 61(1995), pp. 154-170, 1995.

[17] R. H. Davies, C. Twining, T. Cootes, J. Waterton, C. Taylor, 3D Statistical Shape Models Using Direct Optimisation of Description Length. ECCV, 3 (2002), pp. 3-20.

[18] S. Meller, E. Nkenke, W. Kalender, Statistical Face Models for the Prediction of Soft-Tissue Deformations After Orthognathic Osteotomies. MICCAI, 2 (2005), pp. 443-450

[19] S. Zachow, H. Lamecker, B. Elsholtz and M. Stiller, Reconstruction of mandibular dysplasia using a statistical 3D shape model. Computer Assisted Radiology and Surgery; Int Congres Series, 1281, (2005), pp 1238-1243.

[20] A. Frangi, F., D. Rueckert, J. A. Schnabel, and W. J. Niessen, Automatic construction of multiple object three-dimensional statistical shape models: Application to cardiac modeling. IEEE Transactions on Medical Imaging, 21.9 (2002), pp.

[21] M. Fleute, S. Lavallée, R. Julliard, Incorporating a statistically based shape model into a system for computer-assisted anterior cruciate ligament surgery. Medical Image Analysis, 3.3 (1999), pp 209-222.

[22] F. L Bookstein. Landmark methods for forms without landmarks: morphometrics of group differences in outline shape. Medical Image Analysis, 1 (1997), pp. 225-243.

[23] W. E. Lorensen, H. E. Cline. Marching cubes: A high resolution 3D surface construction algorithm. Computer Graphics, 21 (1987), pp. 163-169.

[24] - decimation

[25] R. A. Banvard, The Visible Human Project® Image Data Set from Inception to Completion and Beyond. CODATA 2002 : Frontiers of scientific and technical data, Track I-D-2: Medical and Health Data, (2002), Montreal, Canada

[26] F. Pighin, J. Hecker, D. Lischinski, R. Szeliski and D. H. Salesin, Synthesizing Realistic Facial Expressions from Photographs. Proceedings of Siggraph, (1998), pp 75-84, Orlando, FL, USA.

[27] S. Buchaillard, S. H. Ong, Y. Payan, K. W. C. Foong, Reconstruction of 3D Tooth Images. Proceedings of ICIP 2004, (2004), pp. 1077-1080.

[28] R. Szeliski, S. Lavallée, Matching 3-D anatomical surfaces with non-rigid deformations using octree-splines. International Journal of Computer Vision, 18 (1996), pp. 171-186.

[29] M. Berar, M. Desvignes, G. Bailly, Y. Payan, 3D meshes registration: application to skull model, Proceedings of the International Conference on Image Analysis and Recognition - ICIAR, (2004), vol. 2.:pp 100-107, Porto, Portugal.

[???] M. Moshfeghi. Elastic Matching of Multimodality Images. Graphical models and Processing, 53 (1991), pp. 271-282.

[30] I. L. Dryden, K. V. Mardia; Statistical Shape Analysis. John Wiley and Sons, London, United Kingdom, 1998

[31] B. Romaniuk , M. Desvignes, M. Revenu, M.-J. Deshayes, Shape Variability and Spatial Relationships Modeling in Statistical Pattern Recognition, 25 (2004) Pattern Recognition Letters, pp. 239-247.

[32] C. Basso, T. Vetter, Statistically Motivated 3D Faces Reconstruction. Proceedings of the 2nd International Conference on Reconstruction of Soft Facial Parts, (2005), pp. 71, Remagen, Germany.

[33] C. Rynn and C. Wilkinson, An appraisal of established and recently proposed relationships between the hard and soft dimensions of the nose in profile. Proceedings of the 2nd International Conference on Reconstruction of Soft Facial Parts, (2005), pp. 35, Remagen, Germany.

Received: December, 2005
Revised: February 2005
Accepted:

Contact address:
Maxime Berar
Laboratoire des Images et des Signaux
961, rue de la Houille Blanche
BP 46
38402 Saint Martin d'Hères
France
e-mail: berar@lis.inpg.fr

Michel Desvignes
Laboratoire des Images et des Signaux
961, rue de la Houille Blanche
BP 46
38402 Saint Martin d'Hères
France
e-mail: michel.desvignes@lis.inpg.fr

Maxime Berar is a doctoral student at LIS, Grenoble. He received an engineer degree in electronics form the "Ecole Nationale Supérieure d'Electronique et de Radioélectricité de Grenoble (ENSERG)" in 2002. His scientific interests include statistical modeling and Kernel methods.

Michel Desvignes is currently professor in computer science at the ENSERG and researcher at LIS. His scientific interests includes image processing and pattern recognition methods.

Gérard Bailly is CNRS researcher since 1986, senior researcher since 1991 and is head of the Talking Machines team at Institute of Speech Communication (ICP), Grenoble.

Yohan Payan is CNRS researcher at The Computer-Aided Surgery group (GMCAO: Gestes Médico-Chirurgicaux Assistés par Ordinateur) of TIMC laboratory, and coordinates the modeling works that are carried out in TIMC.
